Revista Mexicana de Física **36** *No. 2(1990) 294–309*

Zero-temperature properties of a spin-polarized atomic hydrogen fluid

M.A. Solís, M. Fortes
Instituto de Física,
Universidad Nacional Autónoma de México,
Apartado postal 20–364, 01000 México, D.F. México

E. Buendía, R. Guardiola
Departamento de Física Moderna, Universidad de Granada,
E–18071 Granada, Spain

C.S. Ho,* M. de Llano
Physics Department, North Dakota State University,
Fargo, North Dakota, 58105, USA

William C. Stwalley
Center for Laser Science and Engineering,
Department of Physics, Astronomy and Department of Chemistry,
University of Iowa, Iowa City, Iowa 52242, USA
(Recibido el 10 de enero de 1990; aceptado el 15 de febrero de 1990)

Abstract. The ground state energy, the pressure and the sound velocity are calculated from first-principles for a wide range of densities in fluid spin-polarized atomic hydrogen. We employ Quantum Thermodynamic Perturbation Theory (QTPT), whereby the interparticle attraction is the perturbation, with two pair-potentials for the spin-polarized state, the Lennard-Jones and Kolos-Wolniewicz forms. Energy calculations reported in the literature agree with ours in the regime of very low density, and for higher densities our calculations are below the variational ones.

PACS: 67.65.+z; 67.40.Kh; 05.30.Jp

I. Introduction

During the past fifteen years, the possibility of producing bulk electron-spin-polarized atomic hydrogen at optimum conditions of density and temperature in order to observe Bose-Einstein (BE) condensation, has captured the interest of both theorists and experimentalists, who have tried to predict and observe the properties of this new quantum system. At very low temperature, it has been possible to produce and

*Present address: Physics Dept., Chung Yuan Christian University, Taiwan 320, Republic of China.

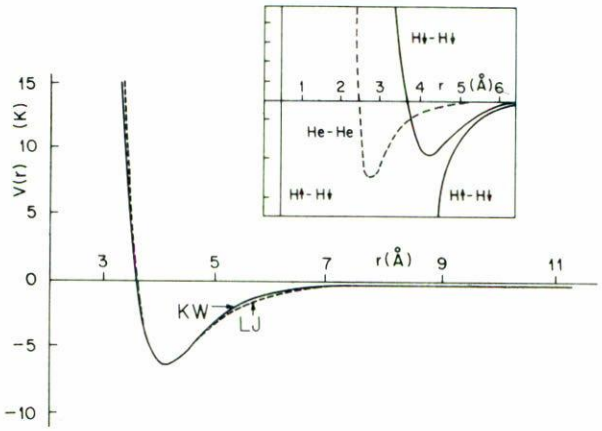

FIGURE 1. Lennard-Jones (LJ) and Kolos–Wolniewicz (KW) potentials between two hydrogen atoms in the triplet electronic state. Inset: The interaction in the singlet and triplet electronic states of hydrogen compared with that of two helium atoms.

store atomic hydrogen by introducing it into a magnetic field of the order of 10 T (tesla). In this way, pairs of atoms are forced to interact via the spin-polarized state $^3\Sigma_u^+$ instead of the singlet $^1\Sigma_g^+$ spin state, the latter [1] being unstable and thus not leading to recombination into molecular H_2. The rapid three-body recombination of hydrogen both in the bulk gas, and particularly when adsorbed on the confining helium surfaces, have unfortunately limited the density thusfar acheived to $\sim 5 \times 10^{18}$ cm^{-3} and heated the gas above the BE critical temperature T_c (in the limit of weakly-interacting bosons $T_c = 3.31\hbar^2\rho^{\frac{2}{3}}/(mk) = 74$ mK at a density of $\rho \cong 10^{19}$ cm^{-3}) [2].

The ground-state properties of atomic hydrogen have been calculated using a wide variety of variational methods [3–5] as a first step to understand this system. In these calculations, it is generally assumed that pair interaction is the $^3\Sigma_u^+$ atomic triplet potential, Fig. 1. At best, the calculated energies —exact in the low-density regime— represent upper bounds to the exact energy.

In this work, we report the energy per atom, the pressure and the sound velocity, as functions of the particle density ρ, for the ground state spin-polarized atomic hydrogen. We use the Quantum Thermodynamic Perturbation Theory (QTPT) recently developed [6] which has been successful in the determination of the ground state energy of ^{4}He since it reproduces the Green-Function-Monte-Carlo (GFMC) [7] results within the statistical errors of the simulations.

In Sec. 2 the QTPT is briefly discussed in a schematic way since detailed accounts have been published elsewhere [6,12,22]. We only discuss the method appropriate for a general bosonic system. In Sec. 3 we apply the QTPT to spin-polarized atomic hydrogen (H↓) and we present our results. Sec. 4 is devoted to conclusions.

2. Quantum thermodynamic perturbation theory

We start with the well-known low-density expansion produced by quantum field perturbation theory [8] for the ground state energy per boson particle

$$\frac{E}{N}(\rho) = \frac{2\pi\hbar^2\rho a}{m}\left[1 + C_1(\rho a^3)^{\frac{1}{2}} + C_2(\rho a^3)\ln(\rho a^3) + \cdots + O(\rho a^3)\right], \tag{1a}$$

where C_1 and C_2 are the pure numbers

$$C_1 = \frac{128}{15\pi^{\frac{1}{2}}}, \qquad C_2 = 8\left(\frac{4\pi}{3} - 3^{\frac{1}{2}}\right),$$

m is the particle mass, which in this case gives

$$\frac{\hbar^2}{m} = 48.133716 \text{ KÅ}^2,$$

ρ is the particle density, and a is the S-wave scattering length associated with the assumed pair interaction. In general, a may be either positive or negative. To avoid imaginary terms in (1a) when $a < 0$, we replace a by its numerical expansion in powers of an appropriately defined "switching" parameter $0 \leq \lambda \leq 1$, associated with the intensity of the attractive part of the potential,

$$V(r) = V_{\text{rep}}(r) + \lambda V_{\text{att}}(r). \tag{2}$$

Thence

$$a = a_0 + a_1\lambda + a_2\lambda^2 + \cdots = a_0\left(\sum_{i=0}^{\infty}\alpha_i\lambda^i\right), \tag{3}$$

with $\alpha_i = a_i/a_0$, $i = 0, 1, \ldots, \infty$.

Substituting (3) into (1a) leaves

$$\frac{E}{N} = \frac{2\pi\hbar^2}{ma_0^2}x^2\sum_{i=0}^{\infty}\alpha_i e_i(x)\lambda^i, \tag{1b}$$

where $x = (\rho a_0^3)^{\frac{1}{2}}$ and

$$e_i(x) = 1 + C_{1i}x + C_{2i}x^2\ln(x^2) + O(x^2). \tag{4}$$

We now have a purely real expression for the energy, even for λ large enough so that a is negative. In (4) the dimensionless coefficients C_{1i} and C_{2i} have been deduced [9] for $i = 1, 2, \ldots, 6$ through the computer algebraic scheme MACSYMA [10]

in terms of C_1, C_2, a_1, $a_2, \ldots, a_6$. Clearly, $C_{10} = C_1$ and $C_{20} = C_2$. The new expression (4) for the energy is a double series: it is irregular in the density ρ, but regular in the attractive intensity parameter λ. Although we have been able to transform the original energy series so as to have real terms only, this is still a low density expansion. Extrapolation of (1*b*) for non-zero x and λ is undoubtedly required for to systems like H↓. Padé [11] and tailing [12] extrapolants will be used here. They have proved [13] considerably successful in reproducing the correct behavior of functions for which only the beginning of an expansion series is available.

Further extrapolations for the density give us the $\epsilon_i(x)$ approximants for $e_i(x)$, with $i = 1, 2, \ldots, 6$, such that the energy per boson, Eq. (1*b*) will transform into

$$\frac{E}{N} = \frac{2\pi\hbar^2}{ma_0^2} x^2 \sum_{i=0}^{\infty} \alpha_i \epsilon_i(x) \lambda^i. \tag{5a}$$

We limit ourselves to 6th order in the power series for λ. The $\epsilon_i(x)$ will be discussed further. For λ different from zero, the extrapolations are calculated using the common Padé approximants. To do this we rewrite Eq. (5*a*) in the following way

$$\frac{E}{N} = \frac{2\pi\hbar^2}{m_0^2} x^2 \epsilon_0(x) \left(\sum_{i=0}^{6} F_i(x) \lambda^i \right), \tag{5b}$$

with $F_i(x) = \frac{\alpha_i \epsilon_i(x)}{\epsilon_0(x)}$ such that the respective λ–Padé approximants give a sequence of approximants to the energy per particle designated by

$$\frac{E}{N} \equiv \frac{2\pi\hbar^2}{ma_0^2} x^2 \epsilon_0(x) [L/M](\lambda), \quad 0 \leq L + M \leq 6. \tag{6}$$

The pair interaction potential $V(r)$ between particles is separated into attractive and repulsive parts within the Classical Thermodynamic Perturbation Scheme according to Barker & Henderson (BH) [14] and Weeks, Chandler & Andersen (WCA) [15], respectively as

$$\theta(\sigma - r)V(r) + \lambda\theta(r - \sigma)V(r), \qquad \text{(BH)} \tag{7}$$

$$\theta(r_m - r)(V(r) + \epsilon) + \lambda(\theta(r - r_m)V(r) - \epsilon\theta(r_m - r), \qquad \text{(WCA)} \tag{8}$$

with $0 \leq \lambda \leq 1$ (Fig. 2). In other words, for a LJ potential the (BH) decomposition is at the zero of the potential, namely σ, while the (WCA) splitting is at the zero of the corresponding force $-dV(r)/dr$, namely at $r_m = 2^{1/6}\sigma$, which is the minimum of the potential. It has been argued [16] that Eq. (7) is appropriate for describing dilute gases while Eq. (8) is more appropriate for dense liquids.

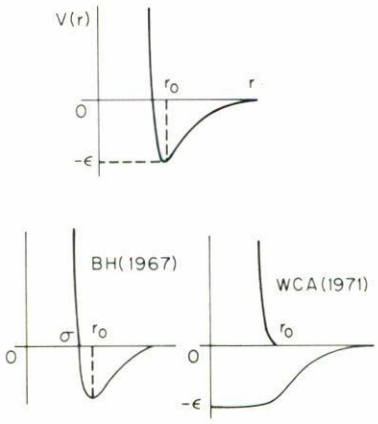

FIGURE 2. Barker-Henderson (BH) and Weeks-Chandler-Andersen (WCA) decomposition of the potential $V(r)$.

As in the earlier classical studies [14,15], the first step consists in an accurate treatment of the purely repulsive fluid. In the low-density limit this is described by Eq. (1*b*) with $\lambda = 0$, namely,

$$\frac{E}{N} \cong \frac{2\pi\hbar^2}{ma_0^2} x^2 e_0(x), \tag{9a}$$

$$e_0(x) = 1 + C_1 x + C_2 x^2 \ln x^2 + O(x^2). \tag{9b}$$

For identical hard spheres, a_0 is just the sphere diameter, and all possible Padé-like approximants $\epsilon_0(x)$ to the series $e_0(x)$ of Eq. (9*b*) have been studied [17,19]. The $\epsilon_0(x)$'s are *defined* so that $\epsilon_0(x) - e_0(x) = O(x^2)$, if a value for the coefficient of the unknown term, say $C_{30}x^2$, is assumed. Of the twelve such extrapolants to $e_0(x)$, only *two* possess acceptable global fits to the boson hard sphere GFMC data [18], each with just one adjustable constant C_{30}. Both forms turn out to be almost coincident with each other from low to moderate densities (physical, *e.g.*, equilibrium liquid ^{4}He, or fluid spin-polarized atomic hydrogen, or alpha matter, etc.), as well as with the GFMC calculations; they begin differing at higher densities. Of the two forms, the approximate having the smallest least-mean-square-fit value with the four available GFMC data points, turns out to be [19]

$$\epsilon_0(x) = \left(1 - \frac{\frac{1}{2}C_1}{1 - \frac{2C_2}{C_1}x(\ln x + [C_{30} - 3C_1^2/4]/(2C_2))}\right)^{\frac{1}{2}}, \tag{10}$$

which gave $C_{30} = 25.110 \pm 0.287$ and a standard deviation of 0.0051 for the fit.

The form (10) when expanded for small x reproduces (9.*b*). It clearly possesses a second-order pole at $x = 0.7245 \pm 0.0045$.

Since a_0 of Eq. (9*b*) scales together with the density ρ as $x = (\rho a_0)^{\frac{1}{2}}$, at low enough densities a fluid of soft spheres with an S–wave scattering length a_0 should behave like a fluid of rigid spheres of diameter a_0. The question is whether this equivalence persists at higher densities, or nearly so. The answer appears to be "yes", even to the extent of postulating that, for all practical purposes, a fluid of soft spheres described by potentials like (7) or (8) with $\lambda = 0$ will possess a finite, ultimate density value at which the system energy-per-particle is essentially infinite. A real divergence definitely occurs for a classical hard sphere fluid, where the ultimate density might just be the random-close-packing (or Bernal, x_B) density empirically found, in experiments [19] with ball-bearings, for example, to occur at a packing fraction very close (to within four digits) to $2/\pi \cong 0.6366$, or at a density of about 86% of the ordered "primitive hexagonal" (closest) packing value of $\rho_0 = 2^{\frac{1}{2}}/c^3$, where c is the rigid sphere diameter. The Bernal density for boson hard spheres, as predicted by (10), is only about 37% of ρ_0, a reduction perhaps attributable to symmetry and quantum effects.

To incorporate the i-th order perturbation corrections, we construct all possible Padé-like approximants $\epsilon_i(x)$ such that $\epsilon_i(x) - e_i(x) = O(x^2)$, where the $e_i(x)$ $(i = 1, 2, \ldots, 6)$ are the two-termed series in Eq. (4). One arrives at four distinct forms, each of which upon expansion for small x give back Eq. (4). These are

i) $1 + C_{1i}x/(1 - C_{2i}x \ln x^2/C_{1i})$,

ii) $(1 - C_{1i}x - C_{2i}x^2 \ln x^2)^{-1}$,

iii) $(1 + C_{2i}x^2 \ln x^2)/(1 - C_{1i}x)$, and

iv) $(1 + C_{1i}x)/(1 - C_{2i}x^2 \ln x^2)$.

The density behavior within the physical interval $0 \lesssim \rho \lesssim \rho_B$ of each form is constrained by the following conditions: 1) Since the perturbation potential is negative, both first- and second-order perturbations to the energy must [17] be non-positive throughout the density interval. 2) The first-order contribution, moreover, must clearly increase monotonically in ρ. 3) In every order, the contribution must be finite; specifically, $\epsilon_i(x)$ forms with vanishing denominators in $0 \lesssim x \lesssim x_B = (\rho_B a_0^3)$ are immediately discarded. The above constraints are rigorous; additional conditions can be imposed on physical grounds as follows: 4) Classical thermodynamic perturbation theory [28,29] suggests that $\epsilon_1(x_B) =$ constant, and $\epsilon_i(x_B) \cong 0$, for $i \geq 2$, namely good Stell-Penrose behaviour. 5) Throughout the physical region, $\epsilon_i(x) > \epsilon_{i+1}(x)$.

3. Results and discussion

We have considered two pair interaction potentials between hydrogen atoms in the spin-polarized triplet state $^3\Sigma_u^+$: Lennard-Jones (LJ), with parameters $\sigma = 3.689$ Å and $\epsilon = 6.464$ K from Ref. [24], and Kolos-Wolsniewicz (KW) [25]. Fig. 1 depicts these potentials and Fig. 2 displays two ways of decomposing them. For either decomposition —(BH) and (WCA)— λ expansion coefficients of (3) have been calculated [24,25] up to 14-th order using double precision for these potentials. The a_i values to sixth order are given in Table I in angstrom units. Applying the selection criteria mentioned at the end of Sec. 2, the optimal approximants $\epsilon_i(x)$ to (4) are, for orders 1 through 6, the forms i, i, i, ii, ii and ii, as defined in Sec. 2 respectively, for either interaction and splitting, we have summarized the analysis in Tables III, where the optimal approximants are marked with asterisks and their coefficients C_{1i} and $C_{2i}, i = 1, \ldots, 6$, are listed in Table II. We display in Fig. 3 these forms for KW (BH) case, and compare against the repulsive sphere zero-order extrapolant $\epsilon_0(x)$.

Note from Fig. 3 that $\epsilon_1(x)$ increases in ρ. Hence, the first-order energy-per-particle in the present (soft-sphere-fluid-based) perturbation scheme is $E_1/N \equiv (2\pi\hbar^2/m)\rho a_1 \epsilon_1 (\rho a_0^3)^{\frac{1}{2}}$, where $a_1 < 0$. This E_1/N will decrease faster in ρ than the familiar [8], exact first-order (ideal-gas-based) perturbation contribution $-2\pi\rho V_0 R^3$ for purely attractive bosons interacting with a rectangular well of depth $-V_0$ and range R. In second order, we have $E_2/N \equiv (2\pi\hbar^2/m)\rho a_2 \epsilon_2 (\rho a_0^3)^{\frac{1}{2}}$ again with $a_2 < 0$. Since $\epsilon_2(x)$ in Fig. 3 is essentially constant in x, E_2/N decreases linearly in ρ, just as does the exact [27] second-order result $-(4\pi/15)\rho V_0^2 R^5$ for rectangular-well bosons in the ideal-gas-based perturbation theory. This kind of comparison cannot be continued since the exact results are well-known [8] to diverge for bosons, order by order, as of third-order, because the unperturbed reference, zero-order state is the zero-momentum, plane wave (ideal Bose gas) state. On the other hand, our soft-sphere-fluid-based perturbation result as of third order is not only finite but also is very close in behavior to that expected from the exactness [28,29] of the first-order thermodynamic perturbation theory as one approaches close packing, namely, $\epsilon_i(x_B) \cong 0$, for $i = 2, 3, \ldots$.

The energies per particle in Eq. (6), with $e_i(x)$ replaced by $\epsilon_i(x)$, Padé-extrapolated in λ, have such rapid convergence that all the sixth-order ($L + M = 6$) Padé approximants deviated little from the [6/0] curve for each interaction. In Fig. 4 we display Eq. (6) as given by the approximants $[L/0]$, $L = 0, \ldots, 6$. (o) refer to the variational calculation of Ref. 5. The insets are two amplifications. Fig. 5 shows a very large amplification of all the sixth-order Padé approximants to the energy for KW (BH) interaction, as well as the fifth-order result [5/0]. For the sake of simplicity, we adopt the Padé [6/0], as our converged equation of state, namely

$$\frac{E}{N}(\rho) = \frac{2\pi\hbar^2}{m a_0^2} x^2 \epsilon_0(x)[6/0](\lambda). \tag{11}$$

		BH	WCA
	i	a_i(Å)	a_i(Å)
LJ	0	2.84129547	2.882743
	1	−1.50783058	−1.507586
	2	−0.476483648	−0.491292
	3	−0.170703769	−0.183180
	4	−0.0619603782	−0.069353
	5	−0.0225296216	−0.026318
	6	−0.0081941821	−0.009991
KW	0	2.72895857	2.787960
	1	−1.35925915	−1.364790
	2	−0.427170825	−0.441966
	3	−0.149354116	−0.162605
	4	−0.0527374815	−0.060640
	5	−0.0186443233	−0.022657
	6	−0.00659229887	−0.008468

TABLE I. Expansion coefficients a_i (in Å units) for the scattering length a, as defined in Eq. (3), for the Lennard-Jones and Kolos-Wolniewicz potentials decomposed according to the BH and WCA methods.

		C_{ji}	1	2	3	4	5	6
LJ	BH	1	12.03605	−3.123486	−10.96471	−15.54253	−16.44992	−12.76649
		2	78.61566	−119.4189	−75.17803	21.0166	133.4027	224.5247
	WCA	1	12.03605	−2.450462	−9.900332	−14.4709	−15.90874	−13.50609
		2	78.61566	−110.627	−75.23029	6.303165	105.2795	191.7065
KW	BH	1	12.03605	−2.271039	−10.28664	−15.20743	−16.62314	−13.68629
		2	78.61566	−108.2831	−79.86681	7.758237	118.0404	214.0963
	WCA	1	12.03605	−1.609827	−8.959857	−13.71298	−15.64701	−14.16162
		2	78.61566	−99.64543	−77.0681	−7.186953	84.02801	169.7419

TABLE II. Coefficients C_{ji} $j = 1, 2$, $i = 1, \ldots, 6$, of the optimum approximants $\epsilon_i(x)$ for the Lennard-Jones and Kolos-Wolniewicz potentials, decomposed according to the BH and WCA methods.

KW (BH)

Form	Approximant	ϵ_1	ϵ_2	ϵ_3	ϵ_4	ϵ_5	ϵ_6
0	$1 + K_1x + K_2x^2 \ln x^2$	*vp*	*bSPb*	*bSPb*	*bSPb*	*bSPb*	*bSPb*
i	$1 + \frac{K_1x}{1+K_2/K_1x \ln x^2}$	*	*	*	*bSPb*	pole at $x = .02$	pole at $x = .01$
ii	$\frac{1}{1-K_1x-K_2x^2 \ln x^2}$	*nmi*	pole at $x = .07$	pole at $x = .05$	*	*	*
iii	$\frac{1+K_2x^2 \ln x^2}{1-k_1x}$	*vp*	*bSPb*	*bSPb*	*bSPb*	*bSPb*	*bSPb*
iv	$\frac{1+K_1x}{1-K_2x^2 \ln x^2}$	*nmi*	pole at $x = .07$	pole at $x = .04$	*bSPb*	*bSPb*	*bSPb*

KW (WCA)

Form	Approximant	ϵ_1	ϵ_2	ϵ_3	ϵ_4	ϵ_5	ϵ_6
0	$1 + K_1x + K_2x^2 \ln x^2$	*vp*	*bSPb*	*bSPb*	*bSPb*	*bSPb*	*bSPb*
i	$1 + \frac{K_1x}{1+K_2/K_1x \ln x^2}$	*	*	*	*bSPb*	pole at $x = .05$	pole at $x = .03$
ii	$\frac{1}{1-K_1x-K_2x^2 \ln x^2}$	*nmi*	pole at $x = .05$	pole at $x = .04$	*	*	*
iii	$\frac{1+K_2x^2 \ln x^2}{1-K_1x}$	*vp*	*bSPb*	*bSPb*	*bSPb*	*bSPb*	*bSPb*
iv	$\frac{1+K_1x}{1-K_2x^2 \ln x^2}$	*nmi*	pole at $x = .05$	pole at $x = .03$	*bSPb*	*bSPb*	*bSPb*

LJ (BH)

Form	Approximant	ϵ_1	ϵ_2	ϵ_3	ϵ_4	ϵ_5	ϵ_6
0	$1 + K_1x + K_2x^2 \ln x^2$	*vp*	*bSPb*	*bSPb*	*bSPb*	*bSPb*	*bSPb*
i	$1 + \frac{K_1x}{1+K_2/K_1x \ln x^2}$	*	*	*	*bSPb*	pole at $x = .02$	pole at $x = .01$
ii	$\frac{1}{1-K_1x-K_2x^2 \ln x^2}$	*nmi*	pole at $x = .05$	pole at $x = .1$	*	*	*
iii	$\frac{1+K_2x^2 \ln x^2}{1-K_1x}$	*vp*	*bSPb*	*bSPb*	*bSPb*	*bSPb*	*bSPb*
iv	$\frac{1+K_1x}{1-K_2x^2 \ln x^2}$	*nmi*	pole at $x = .04$	pole at $x = .06$	*bSPb*	*bSPb*	*bSPb*

LJ (WCA)

Form	Approximant	ϵ_1	ϵ_2	ϵ_3	ϵ_4	ϵ_5	ϵ_6
0	$1 + K_1x + K_2x^2 \ln x^2$	*vp*	*bSPb*	*bSPb*	*bSPb*	*bSPb*	*bSPb*
i	$1 + \frac{K_1x}{1+K_2/K_1x \ln x^2}$	*	*	*	*bSPb*	pole at $x = .02$	pole at $x = .01$
ii	$\frac{1}{1-K_1x-K_2x^2 \ln x^2}$	*nmi*	pole at $x = .05$	pole at $x = .1$	*	*	*
iii	$\frac{1+K_2x^2 \ln x^2}{1-K_1x}$	*vp*	*bSPb*	*bSPb*	*bSPb*	*bSPb*	*bSPb*
iv	$\frac{1+K_1x}{1-K_2x^2 \ln x^2}$	*nmi*	pole at $x = .04$	pole at $x = .06$	*bSPb*	*bSPb*	*bSPb*

TABLE III. Summaries from the density series analyses to determine the optimum approximants $\epsilon_i(x)$, which are marked with asterisks, for the Lennard-Jones and Kolos-Wolniewicz potentials, decomposed according to the BH and WCA methods. Abbreviations used: *vp* ≡ violates positivity; *nmi* ≡ non monotonically increasing; *bSPb* ≡ bad Stell-Penrose behavior.

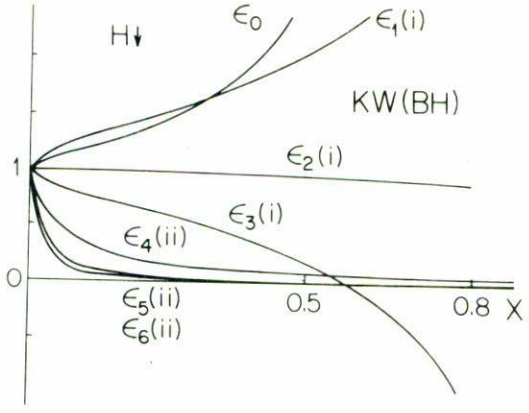

FIGURE 3. Optimum approximants $\epsilon_i(x)$, $i = 1, \ldots, 6$ from the analysis for the KW potential with the decomposition according the BH method. The roman number in parenthesis indicates the form of the approximant used among the four defined in Sec. 2. Also displayed is the approximant $\epsilon_0(x)$ for the energy of the hard sphere fluid Eq. (10).

In Fig. 6 we show this energy for each interaction and splitting within the density range [1 to 100] $\times 10^{-4}$ Å^{-3}. Also shown are the results from several variational calculations, as indicated. Fig. 7 illustrates these results in the density range [1 to 20] $\times 10^{-4}$ Å^{-3}. At such low densities our results agree very well with all variational calculations reported in the literature. At higher densities our results are *below* these given by Miller & Nosanow (M&N) and variational Monte Carlo (MC). Similar calculations [6] with the QTPT for the ^{4}He liquid system agree with Green Function Monte Carlo (GFMC) calculations within the statistical errors of the simulation. It would be very good to have experimental results to compare with. For these densities the importance of the repulsive part of the potential is well known. In our case, as the hard sphere diameter increases, the energy per boson for a given density increases too.

The pressure $P(\rho)$ and the sound velocity $v_s(\rho)$ for the system, as a function of the density are obtained from Eq. (11) through the following thermodynamic relations

$$P(\rho) = \rho^2 \frac{d[E(\rho)/N]}{d\rho}, \tag{12}$$

$$mv_s^2 = \frac{d[P(\rho)]}{d\rho}. \tag{13}$$

The derivatives were performed with the computer algebraic program REDUCE [30].

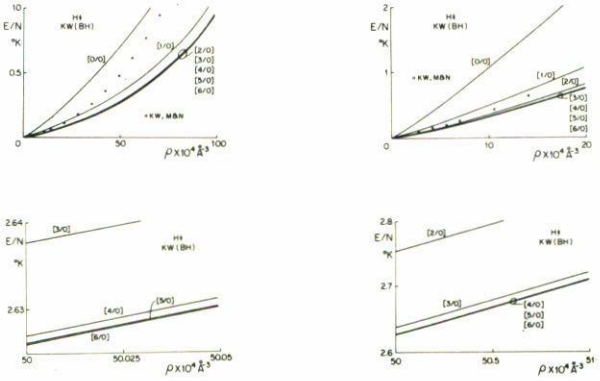

FIGURE 4. Convergence of Padé approximants [L/0], $L = 1, \ldots, 6$, for the energy per hydrogen atom as a function of density, for the KW potential and the BH decomposition. The (o) are the results for Miller & Nosanow for the same system and potential. Inset: Three different amplifications.

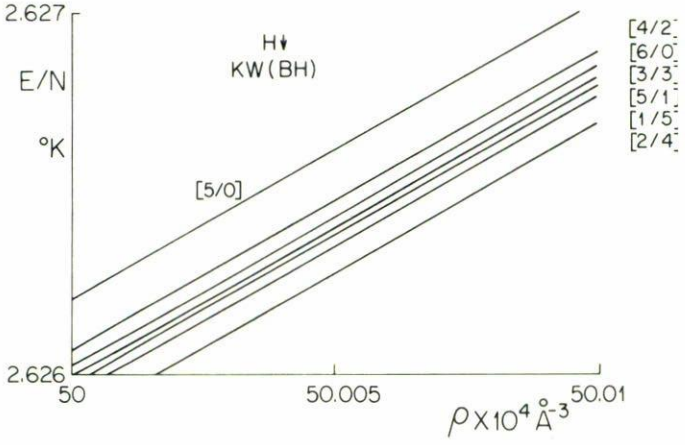

FIGURE 5. Amplification of Padé approximants of 6th order for the energy per hydrogen atom for the KW interaction with BH decomposition. The strip on which all these approximants fall is only ~ 0.2 mK.

Our results for the pressure are shown in Figs. 8 and 9, and for the sound velocity given in Figs. 10 and 11, for densities within the same ranges in which the energy E/N was given. In these figures we also show the results for the few existent other calculations. In Fig. 11 the crosses denote results of Lantto & Nieminen for the KW potential. In Fig. 8 we do not observe the fluid-solid phase transition predicted in Ref. [24] at a density of $\rho = 65$ cm^3/mole $= 92.6 \times 10^{-4}$ Å^{-3} and a pressure of the

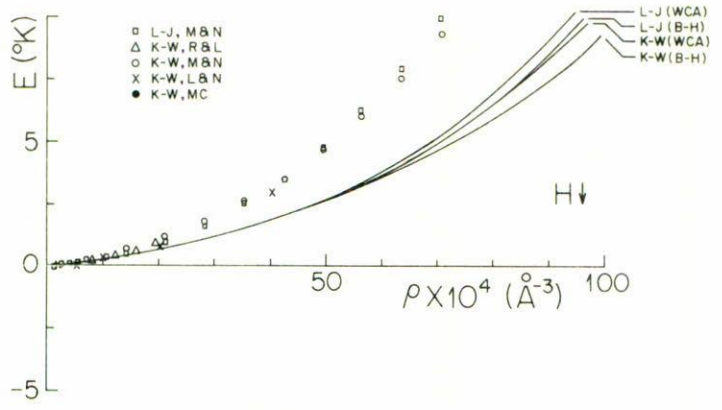

FIGURE 6. Energy curves per hydrogen atom for LJ and KW potentials, decomposed according to the BH and WCA methods. (□) Variational results of Miller & Nosanow for the LJ potential; (○) same for the KW potential; (Δ) variational results of Ristig & Lam [3] for the KW potential; (×) results of Lantto & Nieminen [3] for KW potential; (•) results of Etters, Danilowicz and Palmer [4] with a variational Monte Carlo method for KW potential data fit to a Morse potential form.

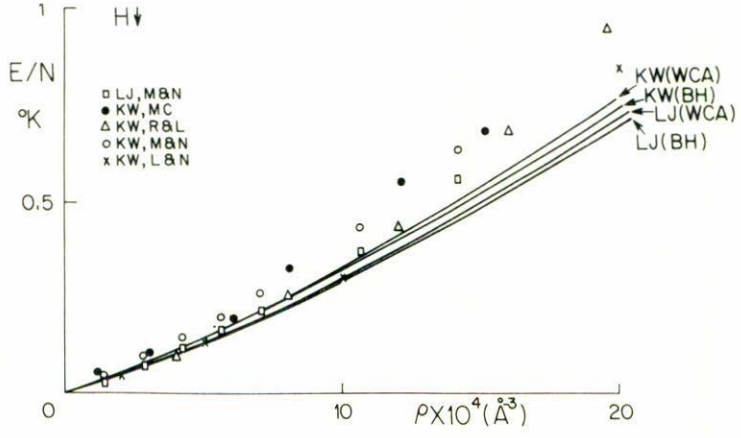

FIGURE 7. Same as Fig. 6 but amplificated in scale.

order of $P = 50$ atm. This may be a limitation in our calculations. Nevertheless, from the same figure we can observe that at this density the system is at a pressure of 21.4, 24.8, 27.7 or 31.1 atm, depending on whether the interaction is KW (BH), KW (WCA), LJ (BH) or LJ (WCA). In the same way, in order to obtain a pressure of 50 atm with (12), densities .010265, .01056, .01090 or .01136 Å^{-3}, respectively, are

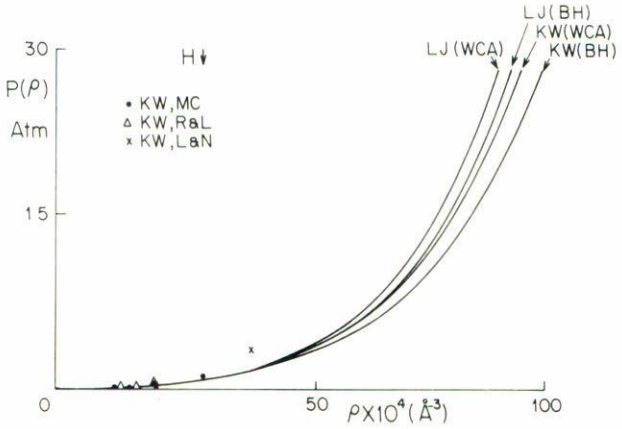

FIGURE 8. Pressure curves as a function of the density, Eq. (12) for LJ and KW potentials decomposed according to the BH and WCA methods. (Δ) results of Ristig & Lam [3] for the KW potential; (×) results of Lantto & Nieminen [3] for the KW potential; (•) results of Etters, Danilowicz and Palmer [4] with a variational Monte Carlo method for KW data fit to a Morse potential form.

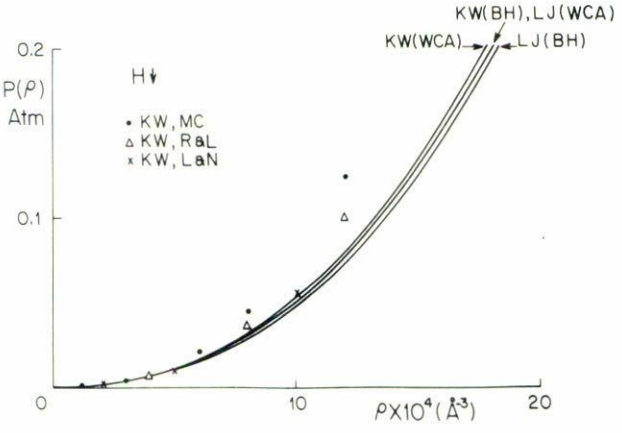

FIGURE 9. Same as Fig. 8 but amplified in scale.

necessary depending on the interaction used, namely LJ (WCA), LJ (BH), KW (WCA) or KW (BH).

4. Conclusions

The low-density (ideal-gas-based) series for the ground-state energy of a many-boson system of particles is rearranged by computer algebra into a double-series. The

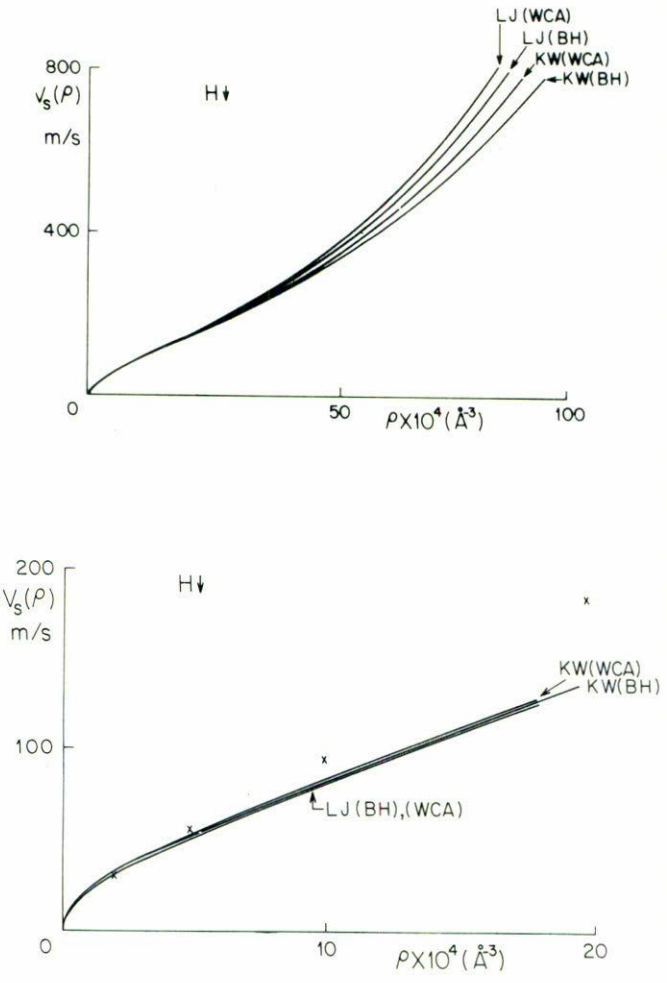

FIGURE 11. Same as Fig. 10 but amplified in scale. The crosses denote results of Lantto & Nieminen [3] for KW potential.

two variables are density and coupling strength of the attractive potential of the pair-interaction. Thus, in analogy to the classical case, one deals with a quantum thermodynamic perturbation theory QTPT in which the unperturbed fluid is not the ideal gas but the fluid of hard- (or soft-) spheres, *and* in which each order correction to this reference fluid is itself a "low-density expression". The latter set of series are extrapolated to higher (*i.e.*, physical) densities through Padé techniques.

Our results agree at very low-densities with all variational calculations carried out on this bosonic fluid, and at higher densities lie everywhere below in energy

as expected. The method should be accurate, in principle, to densities high enough that the variational descriptions will break down.

References

1. I.F. Silvera and J.T. Walraven, *Phys. Rev. Lett.* **44** (1980) 164.
2. J.D. Gillaspy and I.F. Silvera, *Phys. Rev.* **B 38** (1988) 9231.
3. L.J. Lantto and R. M. Nieminen, *J. Low Temp. Phys.* **37** (1979) 1; M.L. Ristig and P.M. Lam, in *Recent Progress in Many Body Theories*, edited by J.G. Zabolitzky, *et. al.* Springer-Verlarg (1982) p. 318.
4. R.D. Etters, R.L. Danilowicz and P.W. Palmer, *J. Low Temp. Phys.* **33** (1978) 305.
5. M.D. Miller and L.H. Nosanow, *Phys. Rev.* **B 15** (1977) 4376.
6. M.A. Solís, V.C. Aguilera-Navarro, M. de Llano and R. Guardiola, *Phys. Rev. Lett.* **59** (1987) 2322; C. Keller, M. de Llano, S.Z. Ren, E. Buendía and R. Guardiola, *Phys. Rev.* **B 40** (1989) 11070.
7. M.H. Kalos, M.A. Lee, P.A. Whitlock and G.V. Chester, *Phys. Rev.* **B 24** (1981) 115.
8. A.L. Fetter and J.D. Walecka, *Quantum Theory of Many-Particle Systems.* McGraw Hill, New York (1971).
9. V.C. Aguilera-Navarro, R. Guardiola, C. Keller, M. de Llano and M. Popovic, *Phys. Rev.* **A 35** (1987) 3901; H.M. Hugenholtz and D. Pines, *Phys. Rev.* **116** (1959) 489.
10. R.H. Rand, *Computer Algebra in Applied Mathematics: An Introduction to MACSYMA.* Pitman, London (1984).
11. G.A. Baker, Jr., and P. Graves-Morris, "Padé Approximants", in *Encycl. of Math. and its Applications*, edited by G.C. Rota, Vols. 13 and 14. Addison-Wesley, New York (1981).
12. M.A. Solís, Ph. D. Thesis, Universidad Nacional Autónoma de México, Facultad de Ciencias, México, D.F. (1987).
13. D S. Gaunt and A. J. Guttmann, in *Phase Transitions and Critical Phenomena*, Vol. 3, ed. by C. Domb and M. S. Green. Academic, New York (1974).
14. J.A. Barker and D. Henderson, *Rev. Mod. Phys.* **48** (1976) 597.
15. H.C. Andersen, D. Chandler and J.D. Weeks, *Adv. Chem. Phys.* **34** (1976) 105.
16. D. Chandler, J. D. Weeks and H. C. Andersen, *Science* **220** (1983) 787.
17. G.A. Baker, Jr., M. de Llano and J. Pineda, *Phys. Rev.* **24** (1981) 6304.
18. M.H. Kalos, D. Levesque and L. Verlet, *Phys. Rev.* **A9** (1974) 2178.
19. V.C. Aguilera-Navarro, S. Ho and M. de Llano, *Phys. Rev.* **A 36** (1987) 5742.
20. G.D. Scott and D.M. Kilgour, *J. Phys.* **D2** (1969) 863; J.L. Finney, *Proc. R. Soc. (London) Ser* **A 319** (1970) 479.
21. D. Levesque and L. Verlet, *Phys. Rev.* **182** (1969) 307.
22. E. Buendía, R. Guardiola and M. de Llano, *Phys. Rev.* **A30** (1984) 941.
23. V.C. Aguilera-Navarro, C. Keller, M. de Llano, R. Guardiola and M. A. Solís, *Cond. Matt. Teories III*, Ed. by J. Arponen. Plenum Press (1987).
24. W.C. Stwalley and L.N. Nosanow, *Phys. Rev. Lett.* **36** (1976) 910.
25. W. Kolos and L. Wolniewicz, *J. Chem. Phys.* **43** (1965) 2429.
26. L.P. Benofy, E. Buendía, R. Guardiola and M. de Llano, *Phys. Rev.* **A33** (1986) 3749.
27. V.J. Emery, J.L. Gammel and F.R.A. Hopgood, *Phys. Rev.* **132** (1963) 10.
28. J.M. Kincaid, G. Stell and C.K. Hall, *J. Chem. Phys.* **65** (1976) 2161.
29. G. Stell and O. Penrose, *Phys. Rev. Lett.* **51** (1983) 1397.
30. A.C. Hearn, *REDUCE, User's Manual.* University of Utah, USA (1975).

Resumen. A partir de primeros principios, se calcula la energía del estado base, la presión y la velocidad del sonido dentro de un intervalo amplio de densidades, para el fluido de átomos de hidrógeno con espines polarizados. Empleamos la Teoría de Perturbaciones Termodinámica Cuántica (QTPT), para la cual la interacción entre las partículas es la perturbación, con dos potenciales de pares para el estado de espines polarizados: Lennard-Jones y Kolos-Wolniewicz. Los cálculos para la energía reportados en la literatura coinciden con los nuestros en el régimen de muy baja densidad y, para densidades más altas, nuestros cálculos se encuentran por debajo de los variacionales.